PNAS
www.pnas.org

Supplementary Information

A Therapeutic Convection Enhanced Macroencapsulation Device for Enhancing β Cell Viability and Insulin Secretion

Kisuk Yang, Eoin D. O'Cearbhaill, Sophie S. Liu, Angela Zhou, Girish D. Chitnis, Allison E. Hamilos, Jun Xu, Mohan K. S. Verma, Jaime A. Giraldo, Yoshimasa Kudo, Eunjee A. Lee, Yuhan Lee, Ramona Pop, Robert Langer, Douglas A. Melton, Dale L. Greiner, Jeffrey M. Karp*

*Corresponding author. Email: jeffkarp@mit.edu

The PDF file includes:

Table of Contents

Supplementary Figures and text

Supplementary Text 1. COMSOL® simulation: Modeling of nutrient transport in static device and ceMED.

The pancreatic islets mainly contain the endocrine cells (α, β, γ, and pancreatic polypeptide-cells) and their main role is to secrete hormones to maintain the blood glucose level in the body. These islets need a constant supply of nutrients and oxygen to generate insulin. To demonstrate the nutrient transport limitations of the TheraCyte^{TM}, we modeled a static macroencapsulation device (MED) and compared its performance *in silico* to convection-enhanced MED (ceMED).

The coupled mass transport equations for glucose, oxygen, and insulin were solved for islets within versions of these devices, modelled in 2D using COMSOL 5.0 multiphysics. The cell chamber (CC) was assumed to be axisymmetric with respect to the HF flow channel to save computational power and assumes 100 % equilibration of the fiber. In this model, the islets are assumed to be perfect spheres that are packed within the capsule and distributed uniformly around the fiber in multilayers. The length of the system [both equilibrium chamber (EqC) and CC: 10 mm], HF diameter (inner diameter, 600 μm), HF wall thickness (100 μm) were based on the prototype design of the device. To modularly demonstrate the effects of capsule expansion, the interior is divided into islet layers. The diameter of islets was assumed as 150 μm and 4 layers of islets are housed between the semipermeable HF and PTFE membrane (double layered). The model accounts for the diffusion of nutrients through the porous membrane of the CC. It assumes oxygenated and glucose-rich environment outside the porous membrane and that the perfusate entering the HF has completely equilibrated with the environment.

In the present model, the encapsulated islets are assumed to consume the nutrient, glucose, and oxygen. They also act as insulin source for both local glucose concentrations and time variation of the glucose concentrations. In the traditional TheraCyte^{TM}-type device, nutrient and oxygen transport to islets take place due to diffusion only, which is a very slow transport process. This slow transport from the periphery of the TheraCyte^{TM} limits the oxygen supply to the inner core of the islets, which leads to hypoxia, loss of functionality, and cell death. Thus, it is necessary to understand the mass transport of oxygen, glucose, and nutrients to the islets in the TheraCyte^{TM}. The current mathematical model focuses on these issues for effective transport of oxygen, glucose, and nutrients to islets and insulin release rate out of TheraCyte^{TM}. It has been reported by Hedeskov *et al.* that insulin release by islets follows a biphasic behavior (1, 2). Here, a square wave pulse of glucose elicits a two-phase release of insulin. The first phase of insulin release (a

transient spike) is followed by a slower second phase. This insulin release rate also depends on oxygen availability and decreases nonlinearly with decreasing oxygen concentration (3, 4). Accordingly, it is necessary to incorporate this biphasic nature of insulin release in this model.

Modeling: In the present model, the islets are modeled to secrete the insulin in response to the local glucose concentration level (c_g) as well as the glucose concentration-time gradient ($\partial c_g/\partial t$). The typical insulin release profile follows a Hill-type sigmoid response as a function of glucose concentration change in the first phase and local glucose concentration in the second phase. As the functionality of the islets depends on nutrients, glucose, and oxygen, the glucose consumption is also incorporated into the model using the Michaelis-Menten type kinetics (5). The availability of oxygen is a limiting factor to maintain islet insulin secretion in response to glucose. In addition, islet death due to hypoxia is another factor. Therefore, a critical oxygen concentration affects cell function and cell viability. In the present model, a total of three concentrations for glucose, oxygen, and insulin respectively (c_g, c_o, c_{in}) are used with their corresponding mass transfer equation. In the absence of convective flow, the mass transfer is taking place due to diffusion only. The equation of mass transport equation is given as:

$$\frac{\partial c_i}{\partial t} + \vec{u} \cdot \nabla c_i = D_i \nabla^2 c_i + R_i$$

Where, c_i denotes the concentration [mol m^{-3}], D_i is the diffusivity constant [$m^2 s^{-1}$], R_i the consumption/release reaction rate [mol $m^{-3} s^{-1}$], i denotes the parameter for glucose, oxygen and insulin in the system, $\vec{u}$ represents the velocity field [$m^2 s^{-1}$] for convection, and ∇ is the standard del operator for the Cartesian coordinate system. In the present study, the two different diffusion coefficients for aqueous media ($D_{i,aq}$) and islet tissue ($D_{i,t}$) with their respective species are used (Table S1). The consumption/release rates in the mass transport equation were assumed to follow Hill-type dependence on their respective concentrations and represented by the generalized Michaelis-Menten kinetics:

$$R_i = R_{max} \frac{c_i^n}{c_i^n + C_{Hf}^n}$$

Where, R_{max} denotes the maximum consumption/release rate, C_{Hf}^{n} concentration corresponds to half of the R_{max}, and n slope constant characterizes the shape of response. The glucose consumption rate for islet is modeled the same Michaelis-Menten kinetics with the respective parameters for glucose.

$$R_g = R_{g,max} \frac{c_g^{n_g}}{c_g^{n_g} + C_{Hf,g}^{n_g}}$$

On the other hand, the oxygen consumption rate for islet is modeled using Michaelis-Menten kinetics with the incorporation of two more parameters ($\varphi_{o,g}$,). The first parameter ($\varphi_{o,g}$) accounts for the increased metabolic demand of oxygen for higher glucose concentrations. The second parameter () accounts for cell death due to hypoxia and represents the condition where oxygen concentration falls below the critical oxygen concentration ($c_{o,cr}$) required by the islet to survive.

$$R_o = R_{o,max} \frac{c_o^{n_o}}{c_o^{n_o} + C_{Hf,o}^{n_o}} \cdot \varphi_{o,g} \cdot \delta\left(c_o > c_{o,cr}\right)$$

While the () is a step-down function, depending on the local oxygen concentration, the ($\varphi_{o,g}$) increases with the metabolic demand along with insulin secretion rate as a function of the glucose concentration and given as:

$$\varphi_{o,g} = \varphi_{sc}\left(\varphi_{base} + \varphi_{meta} \frac{c_g^{n_{i2,g}}}{c_g^{n_{i2,g}} + C_{Hf,in2,g}^{n_{i2,g}}}\right)$$

The value of ($\varphi_{sc}, \varphi_{base}, \varphi_{meta}$) are taken from the Buchwald *et al.* (54, 56) to calculate the increased metabolic demand.

The insulin secretion rate depends on the local glucose and oxygen concentrations. To capture the biphasic behavior of the insulin secretion for a step input glucose response, the insulin release is modeled as first phase ($R_{in,Ph1}$) and second phase ($R_{in,Ph2}$) release rates as given below:

$$R_{in,ph1} = R_{in,max,Ph1} \frac{\left(\frac{\partial c_g}{\partial t}\right)^{n_{Ph1}}}{\left(\frac{\partial c_g}{\partial t}\right)^{n_{Ph1}} + C_{Hf,g,Ph1}^{n_{Ph1}}} \cdot \left(\frac{4c_g^4 c_m^4}{\left(c_g^4 + c_m^4\right)^2}\right)$$

$$R_{in,ph2} = R_{in,max,Ph2} \frac{c_g^{n_{Ph2}}}{c_g^{n_{Ph2}} + C_{Hf,g,Ph2}^{n_{Ph2}}}$$

While the insulin released during one glucose cycle is given as sum of the first and second phase release, the insulin release ($R_{in,Ph1} + R_{in,Ph2}$) is multiplied by a modulating factor to limit the insulin release for a local oxygen concentration that is below ~6 μM.

$$R_{in} = \left(R_{in,Ph1} + R_{in,Ph2}\right) \cdot \left(\frac{c_o^3}{c_o^3 + C_{Hf,o,in}^3}\right)$$

Furthermore, to match the correct time scale of the insulin release, a local compartment is added to facilitate the sustained release to a glucose response by following first order kinetics.

$$\frac{dc_{inL}}{dt} = R_{in} - k_{inL}(c_{inL} - c_{in})$$

The velocity field $\vec{u}$ for the convection is calculated using the continuity and Navier-Stokes equations for Newtonian incompressible fluid.

$$\nabla \cdot \vec{u} = 0$$

$$\rho\left(\frac{\partial \vec{u}}{\partial t} + \vec{u} \cdot \nabla \vec{u}\right) = -\nabla p + \mu \nabla^2 \vec{u}$$

Here, ρ denotes density [kg m^{-3}], μ viscosity [kg $m^{-1}s^{-1}$], and p pressure [kg m s^{-2}]. In the present study, the body force term is omitted in the Navier-Stokes due to small size of the device.

Geometry and meshing: The present device is modeled as a 2D device to save on computation cost and model efficiency. A 2D geometry is created with spherical islets of 150 μm diameters placed inside it. The device dimensions are given in the scheme below. For meshing, COMSOL's default "extra fine mesh" option was used to generate the device mesh with 90,000 ~ 110,000 elements and minimum element size of 1.2 μm.

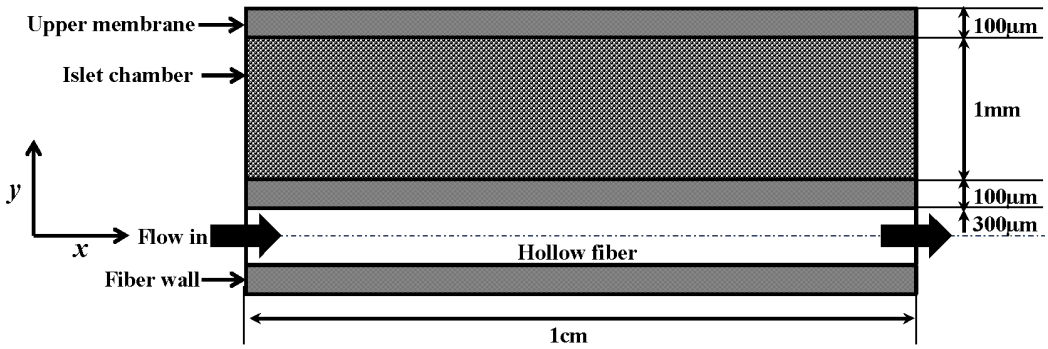

Parameter settings: The parameters used to model the convection flow, islet's nutrient consumption, and insulin secretion rates with their respective units are provided in Table S1 below. Although silicone tubing is used during perfusion due to robust oxygen diffusion characteristics, they were not included in the islet model as it is not the part of the CC.

Parameter	Value
Fiber inner radius	300e-6[m]
Fiber membrane thickness	100e-6[m]
Fiber length	0.01[m]
Cell "Islet" chamber height	2e-3[m]
Cell "Islet" chamber length	0.01[m]
Inlet velocity (V_{max})	0.0001[m/s]
Inlet glucose concentration ($C_{g,\,inlet}$)	1.0 [mol/m^3]
Inlet oxygen concentration ($C_{o,\,inlet}$)	0.2 [mol/m^3]
Inlet insulin concentration ($C_{in,\,inlet}$)	0.0 [mol/m^3]
Diffusivity of glucose in the aqueous media ($D_{g,aq}$)	9e-10 [m^2/s]
Diffusivity of glucose in the islet tissue ($D_{g,\,t}$)	3e-10 [m^2/s]
Diffusivity of oxygen in the aqueous media ($D_{o,aq}$)	3e-9 [m^2/s]
Diffusivity of oxygen in the islet tissue ($D_{o,\,t}$)	2e-9 [m^2/s]
Diffusivity of insulin in the aqueous media ($D_{in,\,aq}$)	1.5e-10 [m^2/s]
Diffusivity of insulin in the islet tissue ($D_{in,t}$)	0.5e-10 [m^2/s]
Glucose consumption rate ($R_{g,\,max}$)	-0.028 [mol m^{-3} s^{-1}]
Oxygen consumption rate ($R_{o,\,max}$)	-0.034 [mol m^{-3} s^{-1}]
Insulin secretion rate ($R_{in,\,max,\,Ph1}$)	21e-5 [mol m^{-3} s^{-1}]
Insulin secretion rate ($R_{in,\,max,\,Ph2}$)	3e-5 [mol m^{-3} s^{-1}]
Glucose Michaelis-Menten constant ($C_{Hf,\,g}$)	10e-3 [mol m^{-3}]
Oxygen Michaelis-Menten constant ($C_{Hf,\,o}$)	1e-3 [mol m^{-3}]
Insulin Michaelis-Menten constant ($C_{Hf,\,g,\,Ph1}$)	0.03 [mol m^{-3} s^{-1}]
Insulin Michaelis-Menten constant ($C_{Hf,\,g,\,Ph2}$)	7.0 [mol m^{-3}]
$C_{Hf,\,o,\,in}$	3e-3 [mol m^{-3}]
$C_{o,\,cr}$	1.0e-4 [mol m^{-3}]
φ_{sc}	1.8
φ_{base}	0.5
φ_{meta}	0.5
C_m	5.0 [mol m^{-3}]
k_{inL}	0.003 [s^{-1}]
n_{Ph1}	2.0

n_{Ph2}	2.5
$n_{i2,\ g}$	2.5
n_o	1
n_g	1
Density of aqueous media (⟩)	998 kg m^{-3}
Viscosity of aqueous media (⌠)	10e-3 Pa.s

Table S1. Parameters used in the present model (4, 6-8).

Boundary conditions: The convection enhanced insulin secretion model is solved using COMSOL metaphysics using flow Free and Porous Media Flow and Transport of dilute species modules. The velocity field is modeled using Navier-Stokes equation for incompressible flow in porous media. The glucose, oxygen, and insulin concentration field are modeled using transport of dilute species modules with convection transport mechanism. The coupled model is implemented in COMSOL 5.0 and solved as time-dependent (transient) problems using PARDISO direct solver for time step of 1.0 s. The simulation was run for 1000 s in order to achieve the steady-state. The following boundary conditions were used for this Navier-Stokes model: the parabolic inflow velocity profile boundary condition at the fiber inlet, a zero pressure boundary condition is used at both fiber outlets as well as at the outside membrane; all other solid walls are described by a no-slip boundary condition. The geometry is assumed to be symmetric along the axis of the fiber, and symmetric velocity boundary condition is used at the center of fiber. For the transport of dilute species modules, the no flux boundary conditions n (-D∇c+cu) = 0 are used for device walls. The inflow for glucose and oxygen concentrations boundary condition are used ($C_{g,inlet}$= 1 mol/m^3, $C_{o,inlet}$= 0.2 mol/m^3, $C_{in,inlet}$= 0.0 mol/m^3). While the insulin concentration was taken as zero at inlet, zero convective flux was used for glucose, oxygen, and insulin at the outlet. The initial boundary condition for glucose and oxygen concentrations used are $C_{g,int}$ = 6.0 mol/m^3, $C_{o,int}$ = 0.2 mol/m^3, $C_{in,int}$ = 0.0 mol/m^3.

Simulations: Simulation of glucose transport into the capsule from the membrane surface revealed that islets immediately adjacent to the membrane receive only 75 ~ 90 % of the concentration of interstitial glucose. The amount of glucose reaching the adjacent islet layers decreases due to metabolic consumption by inner layers of islets with the thickness of the chamber. Consequently, even islets within optimal static MEDs do not receive the interstitial concentrations of nutrients, which may negatively impact their ability to physiologically respond to blood glucose levels. Simulation of oxygen transport revealed hypoxic conditions,

even for those islets situated at the membrane surfaces (< 25 % of interstitial oxygen concentration). If the device chamber is increased in size, interior islet layers receive < 0.0001 mM of oxygen, resulting in decreased function and cell death. Both glucose and oxygen concentrations influence the amount of insulin secretion by encapsulated islets. The static model demonstrates negligible insulin secretion by any islets not situated adjacent to the membrane surface.

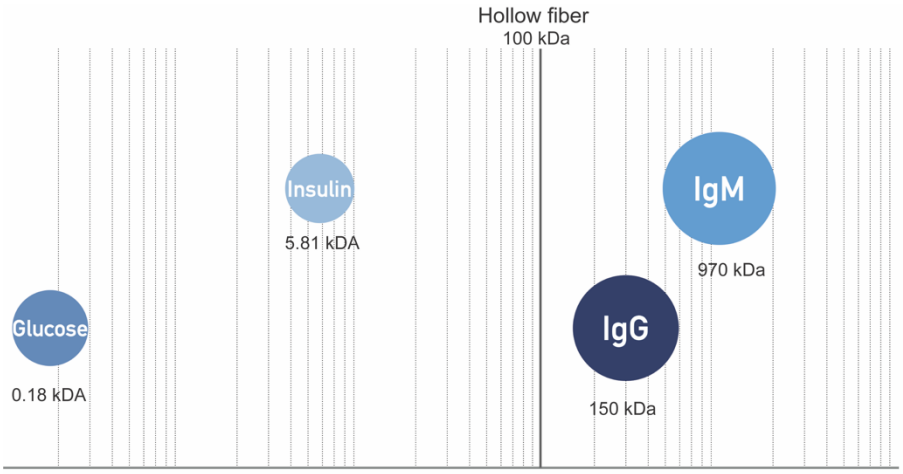

Fig. S1. Selection of a hollow fiber (HF) with 100 kDa molecular weight cut-off allows for exchange of glucose and insulin while also protecting against passage of immunoglobins.

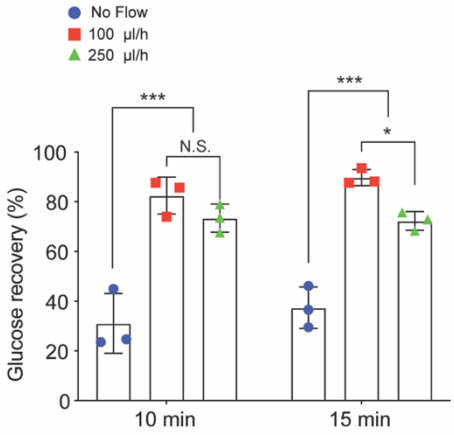

Fig. S2. Flow rates at 100 and 250 µL/h showed no significant difference with regards to glucose recovery percentage in the cell chamber (CC) after 10 min, but showed significant difference after 15 min equilibrium *in vitro* (n=3, ***P<0.001, *P<0.05). N.S., not significant.

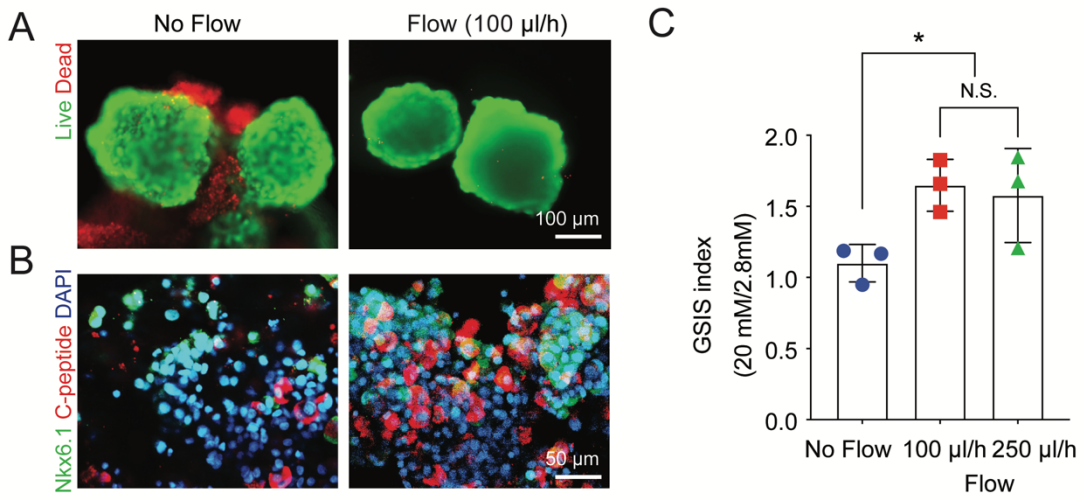

Fig. S3. ceMED shows increased viability and glucose-stimulated insulin secretion (GSIS) indices of encapsulated stem cell derived β clusters (SCβCs).
(A) The viability of cells embedded in alginate gel in the core of ceMED (near HF) was evaluated using a LIVE DEAD kit after 3 days in culture.
(B) Immunofluorescent images of SCβCs from the core of a CC expressed Nkx6.1 and C-peptide after 7 days in culture.
(C) Cumulative GSIS indices from the SCβCs are significantly induced in the flow groups (100 and 250 µL/h) compared to the no flow group (n=3, *P<0.05 *versus* no flow group).

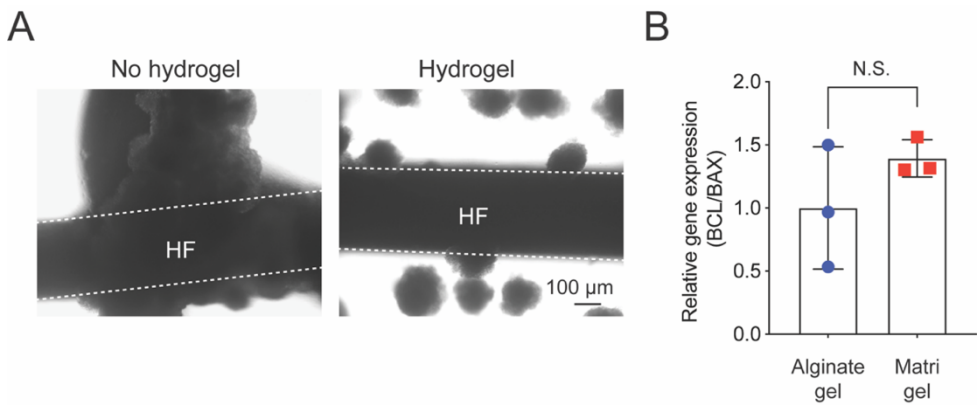

Fig. S4. SCβCs embedded in hydrogel with perfused flow.
(A) Gross morphology of SCβCs in the CC with and without hydrogel. SCβCs generate large aggregates without hydrogel after 3 days in culture.
(B) Gene expression profiles of anti-apoptotic (BCL2) and pro-apoptotic (BAX) (normalized to GAPDH) in SCβCs embedded in alginate gel and Matrigel (n=3) after 2 days in culture.

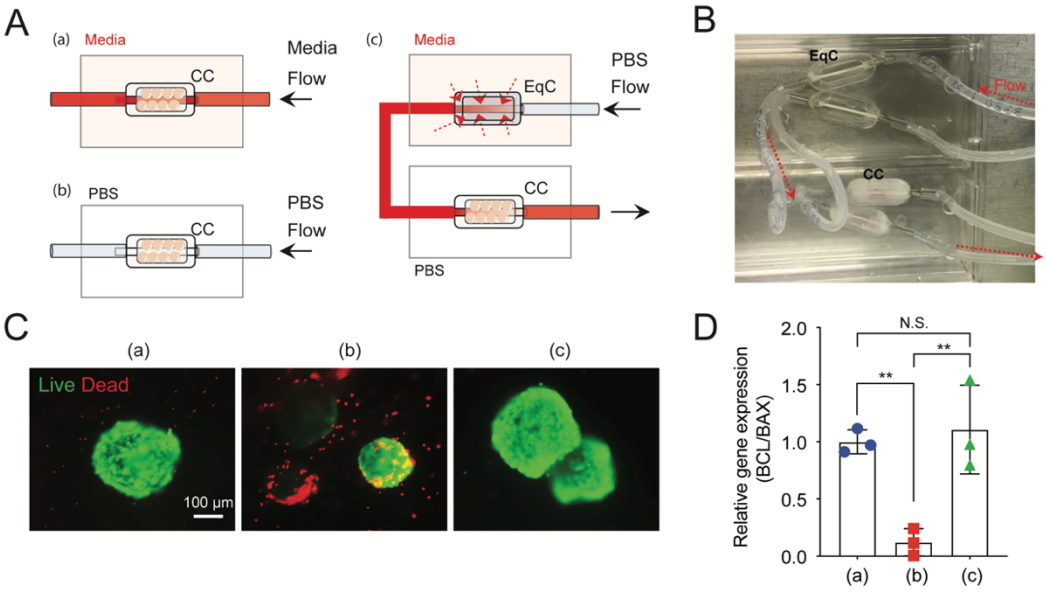

Fig. S5. Perfused flow through equilibrium chamber (EqC) can increase SCβC viability.
(A) Schematic images of SCβCs embedded in Matrigel loaded in CC for 3 experimental groups. (a) the CC is perfused with and submerged in SCβC culture media (positive control). (b) the CC is perfused with and submerged in phosphate-buffered saline (PBS) (negative control). (c) the CC is submerged in PBS and connected to an EqC which is submerged in culture media in a separate chamber and perfused with PBS.
(B) Gross view of *in vitro* setup of experimental group (c).
(C) LIVE DEAD assay shows the importance of EqC for SCβC viability in the CC.
(D) Gene expression ratio of BCL2 and BAX at day 3 in SCβCs loaded in CCs from (a) ~ (c) [n=3, **P<0.01 *versus* (b)].

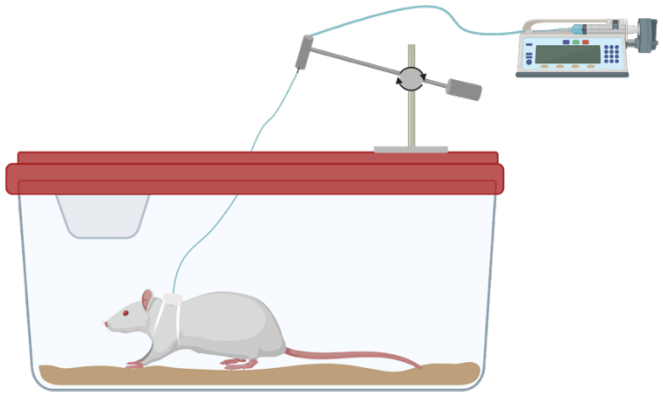

Fig. S6. Animal swivel cage set-up, consisting of an external syringe pump which accurately controls the flow rate. The tether system allows for continuous infusion into subcutaneously transplanted ceMED in live, active animals subcutaneously transplanted with ceMED. *Image created with: Biorender.com*

Supplementary Text 2. Swivel cage set-up.

All animal experiments were performed under the approved Institutional Animal Care and Use Committee (IACUC) protocol by the Center of Comparative Medicine (CCM) at Brigham and Women's Hospital (Harvard Medical School). To enable unobstructed infusion into the transplanted devices and to prevent

interference from animal movements, each animal was singly housed and tethered under the swivel cage set-up. This setting allowed continuous fluid infusion into the subcutaneously transplanted device and convenient collection of equilibrated outflow fluid for glucose content analysis. The tethered system consisted of a harness, a spring tether, a two-channel swivel, a swivel mount, extension tubing which were all purchased from Instech Laboratories (Plymouth Meeting, PA, USA), and a syringe pump (NE-1600, New Era Pump Systems, Farmingdale, NY, USA). The adjustable harness, worn around the forelimbs of the animal, was connected to the stainless steel spring tether which protects the device tubing and transmits rotary movement to the swivel which was clamped onto the counter-balanced swivel mount positioned on top of the rat cage. The extension tubing was connected to the syringe pump.

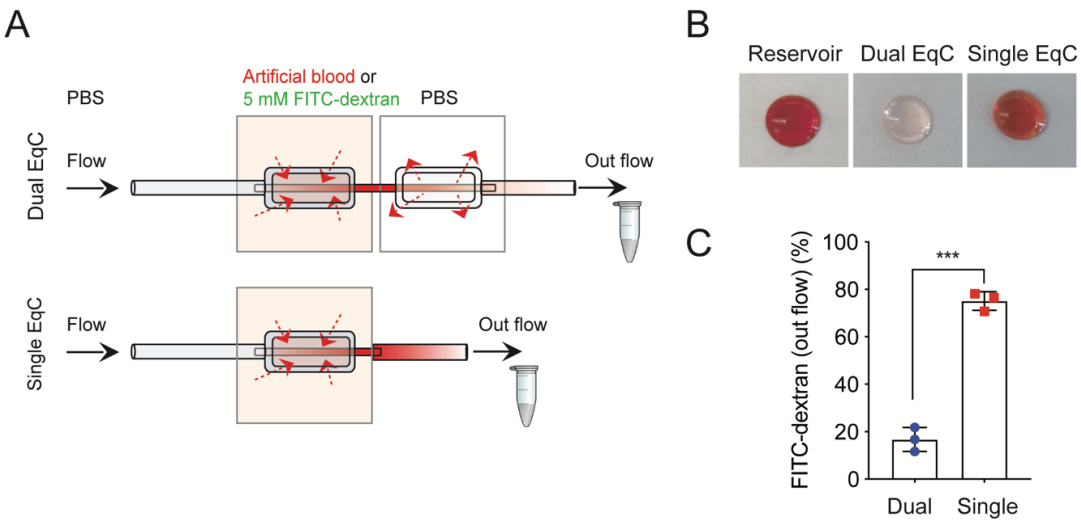

Fig. S7. Dual EqC can increase equilibration and reduce outflow recovery.
(A) Pilot experiment setup comparing single EqC and dual EqC at 250 µL/h flow. The first EqC is submerged in artificial blood to visualize outflow or FITC-dextran (4 kDa) to quantify recovery. The second EqC is submerged in PBS.
(B) Visualization of outflow using artificial blood shows dramatic color loss in the dual EqC group.
(C) The dual EqC reduces outflow FITC-dextran recovery compared to the single EqC (n=3, ***P<0.001 *versus* single EqC group).

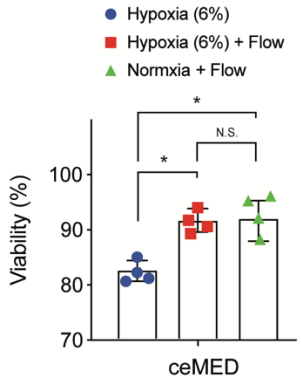

Fig. S8. Perfusate flow supports cell viability in ceMED even under mildly hypoxic condition. Cell viability of MIN6 cells (10 IEQ/μL) (1.5×10^4 cells/μL, assuming 1,500 cells=1 IEQ) at day 2 embedded in alginate gel in the dual EqC ceMED were compared under normoxic *versus* hypoxic conditions. The hypoxic condition mimics the subcutaneous environment *in vivo* (n=4, *P<0.05, *versus* no flow group). The perfusate showed a significant rescue of cell viability under hypoxic condition.

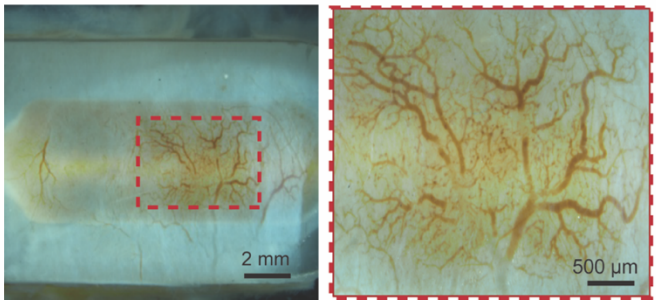

Fig. S9. Subcutaneously transplanted ceMEDs show presence of blood vessels on the surface after 14 days of implantation.

Supplementary Text 3. Device transplantation.

Immunocompetent Lewis Rat (LEW/Crl), 10 ~ 12 weeks old, were purchased from Charles River Laboratory (Wilmington, MA, USA) and used as recipients. Animals were anesthetized with vaporized isoflurane in oxygen (3 % for induction, 1 % for maintenance). Areas on the dorsal region were shaved and prepared with povidone-iodine and ethanol wipes. Animals were given preemptive analgesics in a single dose of 5 mg/kg Meloxicam (Patterson Veterinary, Greeley, CO, USA) delivered subcutaneously. An incision less than 2 cm was made along the midline of the prepared dorsal region to create an opening into the subcutaneous space and a pair of blunt-end scissors was used to create a subcutaneous pocket for the device. A small incision was made at the other end of the pocket to act as the exit port. The devices (seeded with cells in the CC) were then removed from sterile containers, threaded through the opening, and placed into the subcutaneous region using two pairs of tweezers. The inlet and outlet silicone tubing were placed through the two incisions

and connected to extension tubing sterilized by ethanol wetting and PBS wash. The incision sites were closed using 3-0 non-absorbable Nylon sutures with reverse-cutting needle (Ethicon, Somerville, NJ, USA) which were removed after 14 days. Sutured skins were cleansed with ethanol wipes and applied with antibacterial ointment prior to putting on the tethered harness for swivel cage set-up.

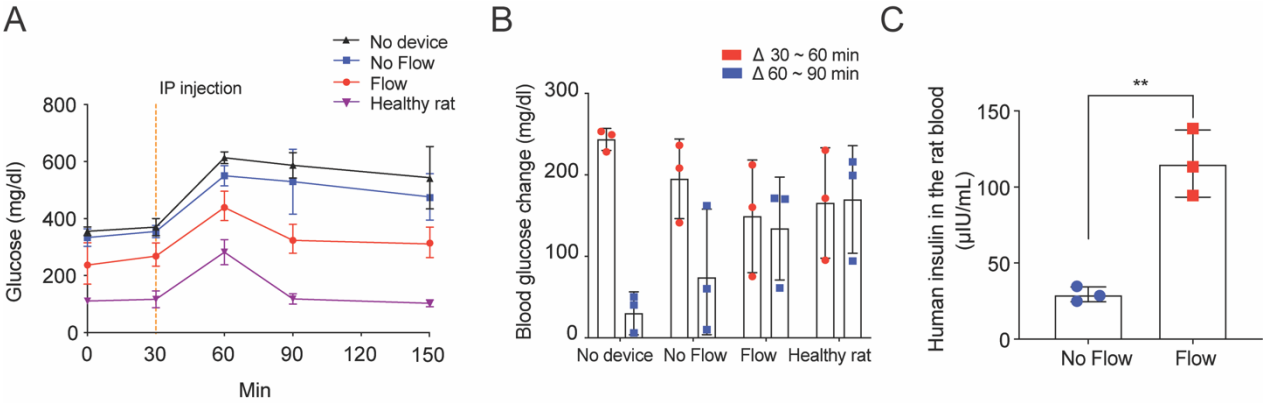

Fig. S10. Subcutaneously transplanted ceMED with human primary islets generates improved glucose tolerance *in vivo*.
(A) Rats showed faster glycemic control after intraperitoneal glucose tolerance test (IPGTT) (2g/kg) when transplanted with ceMED (n=3~4 rats).
(B) Change in blood glucose from 30 - 60 min is higher in no device and no flow transplanted rats compared to rats transplanted with ceMED. Decrease in blood glucose levels from peak blood glucose to 30 min after (60~90 min) IP injection, is greater in flow groups compared to no flow and no device group (n=3 rats).
(C) Human insulin levels detected following the transplantation is higher in flow group compared to no flow (n=3 rats, **P< 0.01 *versus* No Flow group).

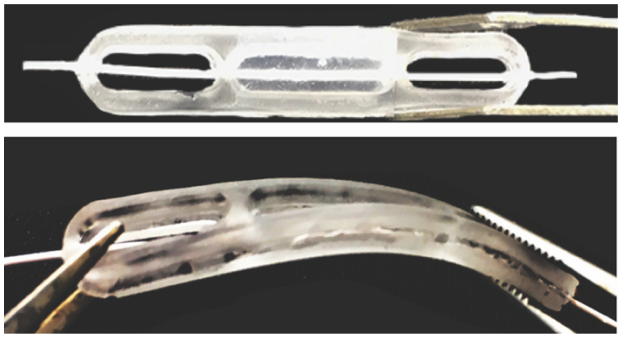

Fig. S11. A polydimethylsiloxane (PDMS) based ceMED can accommodate for cryo-sectioning and surgical implantation.

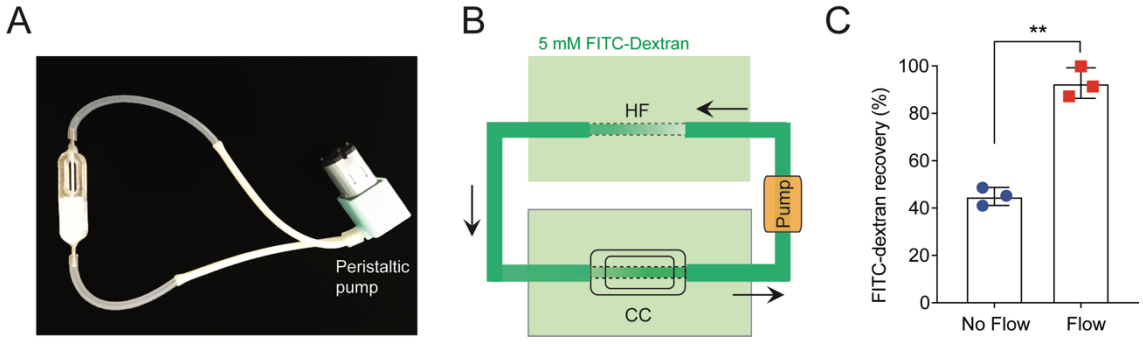

Fig. S12. A closed-loop recirculation system using a peristaltic pump.
(A) Gross view of a closed-loop recirculation system.
(B) Schematic illustration of experimental set up for measuring equilibration of CC in a closed-loop system.
(C) Perfused flow using peristaltic pump increased FITC-dextran (4 kDa) equilibration in the CC compared to no flow group (n=3, **P<0.01 *versus* No flow).

Supplementary Text 4. A closed-loop recirculation ceMED system for long-term treatment.

To eliminate the need for an external pump or the combination of an internal pump with a reservoir that needs periodic replenishment, we performed a benchtop validation of the use of a peristaltic pump and rewiring of the fluidic circuit to enable recirculatory convective flow through the CC. Some one-way implantable pumps (e.g., Medtronics's Synchromed II™ and Flowonix's Prometra II™) are available for use and should allow the implantation of the device subcutaneously. However, limitations of a one-way system include the need for a fluid reservoir which require frequent refills at high flow rates and the formation of edema as a result of the imbalanced absorption rate of interstitium to fluid flow rate. Based on the challenges associated with an one-way system, we seek to develop a closed loop recirculation system using a recirculating pump (e.g., peristaltic pump) considering the long-term application of the ceMED (*SI Appendix*, Fig. 12A). To test such a system, we placed the EqC and CC in two separate reservoirs with 10 mL with a FITC-dextran (4 kDa) (5 mM) (*SI Appendix,* Fig. 12B). Then, the fluid from the CC was collected to investigate its concentration using a microplate reader. Excitation and emission wavelength of 490 nm and 525 nm were used. After 15 minutes, the diffusion-based device (No flow) had 44.9 ± 3.8 % equilibration, whereas the perfusion group with peristaltic pump showed 92.8 ± 6.5 % equilibration (*SI Appendix*, Fig. 12C). This result indicates that the ceMED with a closed loop system can afford equilibration with the surrounding solution.

References

1. B. Vasir, L. P. Aiello, K. H. Yoon, R. R. Quickel, S. Bonner-Weir, G. C. Weir, Hypoxia induces vascular endothelial growth factor gene and protein expression in cultured rat islet cells. *Diabetes* **47**, 1894-1903 (1998).
2. C. J. Hedeskov, Mechanism of glucose-induced insulin secretion. *Physiol. Rev.* **60**, 442-509 (1980).
3. P. Rorsman, L. Eliasson, E. Renström, J. Gromada, S. Barg, S. Göpel, The Cell Physiology of Biphasic Insulin Secretion. *Physiology* **15**, 72-77 (2000).
4. K. E. Dionne, C. K. Colton, M. L. Yarmush, Effect of hypoxia on insulin secretion by isolated rat and canine islets of Langerhans. *Diabetes* **42**, 12-21 (1993).
5. P. Buchwald, FEM-based oxygen consumption and cell viability models for avascular pancreatic islets. *Theor. Biol. Med. Model.* **6**, 5 (2009).
6. L. Michaelis, M. L. Menten, K. A. Johnson, R. S. Goody, The original Michaelis constant: translation of the 1913 Michaelis-Menten paper. *Biochemistry* **50**, 8264-8269 (2011).
7. P. Buchwald, A local glucose-and oxygen concentration-based insulin secretion model for pancreatic islets. *Theor. Biol. Med. Model.* **8**, 20 (2011).
8. P. Buchwald, S. R. Cechin, J. D. Weaver, C. L. Stabler, Experimental evaluation and computational modeling of the effects of encapsulation on the time-profile of glucose-stimulated insulin release of pancreatic islets. *BioMed. Eng. OnLine* **14**, 28 (2015).